Exploitation of Nano-Crystalline Cupric Cxide (CuO) Doped Zinc Oxide (ZnO) Multilayer Thick Film as a CO$_2$ Gas Sensor

*Mankar S.S., **Lamdhade G.T., **Raulkar K.B

*Department of Physics, Shivramji Moghe Arts, Commerce and Science College, Kelapur, Pandharkawada , Dist. Yavatmal, M.S., India
**Department of Physics, Vidya Bharati Mahavidyalaya, CK Naidu Road, Amravati, M.S., India

ABSTRACT

Cupric oxide and Zinc oxide nano-crystalline powder were synthesized via liquid-phase method. The samples are prepared in the form of multilayer thick films. The XRD pattern of (CuO-ZnO) system samples show nanocrystalline form and found the desired peaks of composites. FESEM study reveals that the grain size of nanometer order and shows nano- porous structure, which leads to exhibit large surface area, stability and highest response to CO$_2$ gas. The response time is faster than recovery time. The sample C3 sensor (15CuO:85ZnO) offers high sensitivity, rapid response and recovery to CO$_2$ gas.

Keywords: *Nanoparticles; CuO-ZnO; multilayer thick films; CO$_2$ Gas Sensors*

INTRODUCTION

Nanoparticles CuO and its composite oxides have potential applications as gas sensor. As compared to bulk materials, nanoparticles of Copper oxide (CuO) show high catalytic activity and selectivity due to their large surface to volume ratio. [1-3]. Quentin Simon et al. 2012 [4] synthesized CuO/ZnO nanocomposites on Al2O3 substrates by a hybrid plasma-assisted approach. Various oxidizing and reducing gases such as O$_3$, CH$_3$CH$_2$OH, and H$_2$ are studied for gas sensing properties of CuO/ZnO nanocomposites. Yalu Chen et al.2013 [5] prepared CuO-ZnO nanostructured p-n junction composite via the hydrothermal method. The gas sensing performance of pure ZnO and CuO-ZnO composite toward n butanol was studied. They show that porous structure allows the target gas molecules diffuse rapidly making chemisorption and the chemical reactions on the p-n junctions more easily. At 220 °C 2.7 times higher sensitivity was obtained for CuO-ZnO composite than that of pure ZnO. Ryan Dula Corpuza and Jason Rayala Albiab 2014 [6] fabricated ZnO and ZnO-CuO composites on a graphite electrode via electrophoretic deposition. Greater surface area, smaller particle sizes and thicker deposits exhibit high gas sensitivity. The addition of CuO in the deposition gives compact and dense surface structure resulted to decrease in sensitivity. The expected increase in sensitivity in the presence of CuO was not attained. Madhavrao K. Deore et al. 2016 [7] prepared CuO-doped ZnO thick films by the screen printing technique. These films were studied for different gases such as CO, Cl$_2$, NH$_3$, Ethanol, H$_2$S and LPG and observed that CuO doped films were more selective to H$_2$S gas against the other test gases showing rapid response and recovery time. The main purpose of this work was to develop CuO doped ZnO, nano-crystalline composites sensors which operate at relatively low temperature and sensitive in low possible detection limit with better sensitivity.

EXPERIMENTAL

In the present work of thesis, we have used liquid phase synthesis method for the synthesis of pristine nano-particles of CuO, ZnO and Al_2O_3 [8-10]. All the chemicals used in this study were of GR grade purchase from Sd-fine, India (purity 99.99%). The chemicals are used without any further purification.
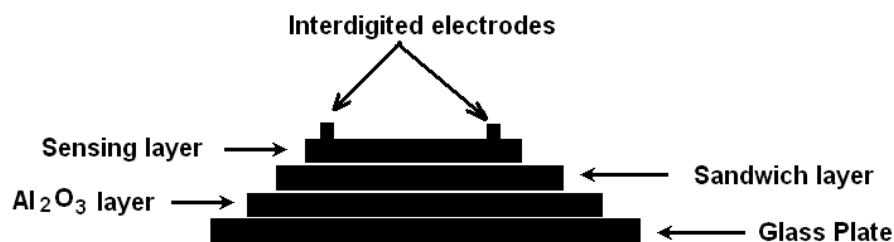
Fabrication of Sensors : Multilayer preparation

Fig.1 Design of multilayer Sensor

On clean glass plate, Al_2O_3 was deposited by using screen-printing technique and it was used as base of the sensor. On Al_2O_3, the sample layers were prepared. Finally on the top, Inter-digited electrodes were fabricated using conducting silver paste and design of multilayer sensor is shown in Fig. 1.

Preparation of Samples of Series: CuO: ZnO / Al₂O₃/GP

The obtained product of fine nanopowder of CuO and ZnO are used for fabrication of thick films sensors by using screen-printing technique. For this, the different X mole% CuO powder (X = 05, 10, 15, 20, 25, 30) was mixed thoroughly with different X mole% of ZnO (X = 95, 90, 85, 80, 75, 70) along with Al_2O_3 base on glass plate (GP) substrate the aid of acetone by using the mortar and pestle. The sample codes, mole% of powder, and thickness are listed in the Table 2.**.** The mixed powder of CuO : ZnO system was further calcinated at temperature 800°C for 5hrs. in the auto-controlled muffle furnace (*Gayatri Scientific, Mumbai, India.*) After, the calcinations again uniformly mixed the powder using the grinder.

Table 1 Thickness of Multi-layers for Series: CuO: ZnO / Al_2O_3/GP Gas Sensors.

Sample Code	Composition	Thickness (x 10^{-4} cm)		
	Layers:----	Upper Layer(1)	Al_2O_3 Layer(2)	Total (1+2)
	Upper /Al₂O₃/Glass plate (GP)			
C1	05CuO:95ZnO/ Al_2O_3/GP	2.8	27.1	29.9
C2	10CuO:90 ZnO / Al_2O_3/GP	3.4	28.7	32.1
C3	15CuO:85 ZnO / Al_2O_3/GP	2.2	29.4	31.6
C4	20CuO:80 ZnO / Al_2O_3/GP	3.9	28.8	32.7
C5	25CuO:75 ZnO / Al_2O_3/GP	2.8	28.9	31.7
C6	30CuO:70 ZnO / Al_2O_3/GP	2.9	30.2	33.1

RESULTS AND DISCUSSION

XRD of CuO & ZnO Nanomaterial and their dopings

The average crystallite size was calculated by Debye-Scherer's equation with the help of XRD patterns as shown in figure 4. The strong and sharp peak of CuO observed at 37° position with (1 1 1) indicates that the sample is having high crystalline quality, and it is in the structure of monoclinic with lattice parameters a = 0.4685 nm, b = 0.3532 nm,

57

and c = 0.5121 nm, which is good agreement with JCPDS card number 88-2341. The average crystalline size was obtained 27 nm from Debye-Scherer's equation, $D = \dfrac{K\lambda}{\beta cos\theta}$

Where, D = nanoparticles crystalline size, K = Scherrer constant (0.98), λ = wavelength and β denotes the full width at half maximum (FWHM).

As shown in figure 2, the XRD pattern peak for CuO doped ZnO exhibits hexagonal and monoclinic crystalline phases at 2θ values of 8.25°, 26.56°, 38.45°, 44.21°, 53.56°, 62.55°, 73.12° and 82.67° (JCPDS Card No.5-3242), with the corresponding planes of (1 0 0), (1 1 0), (1 1 1), (2 2 0), (1 0 2), (2 0 2), (1 0 3), and (1 0 2), respectively. As shown in table 2, Sample Code C3 i.e. (15CuO:85ZnO) sample shows small crystalline size. The average crystalline size was found to be smaller in case of C3 sample and hence its active surface is more [11].
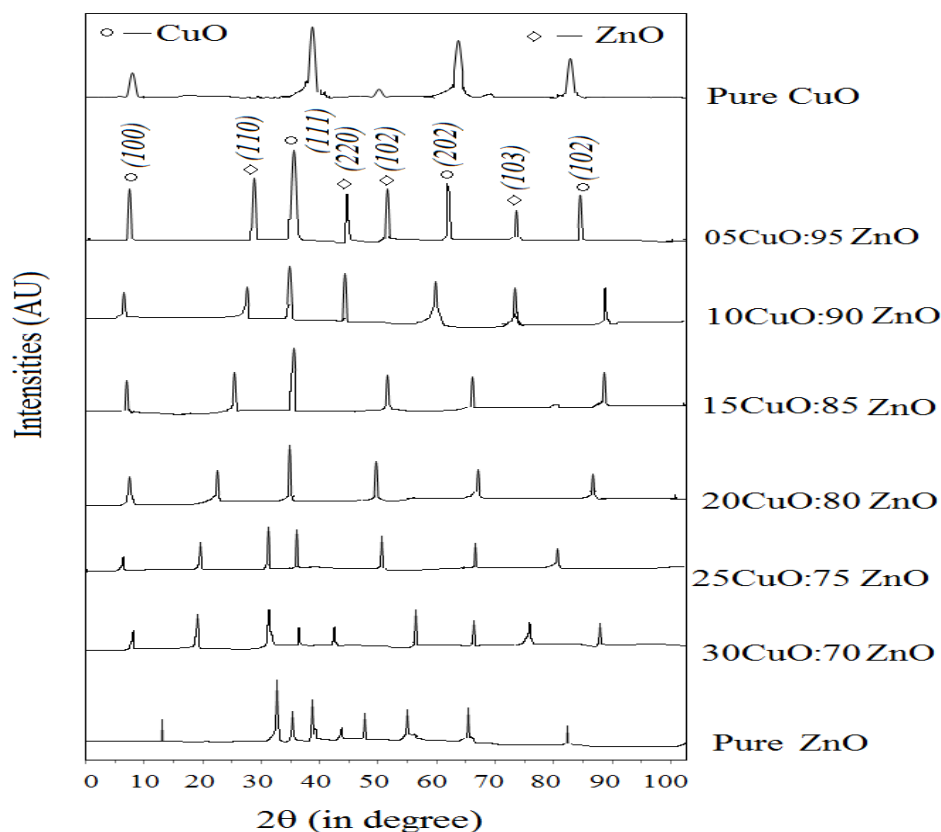

Fig.2. XRD spectra of Pure CuO, Pure ZnO and CuO doped with ZnO Nanomaterial

Table 2 Average crystallite size of ZnO and CuO doped ZnO

Sample Code	Chemical Composition of CuO:ZnO (mole %)	Maximum Intensity Peak Position (2θ) degree	FWHM (2θ) degree	Average Crystallite Size (D) in nm
PC	Pure CuO	43.32	0.1865	162.22
C1	05CuO:95 ZnO	26.45	0.1786	102.33
C2	10CuO:90 ZnO	28.44	0.1862	98.22
C3	**15CuO:85 ZnO**	**29.34**	**0.1372**	**78.33**
C4	20CuO:80 ZnO	32.45	0.1672	93.23
C5	25CuO:75 ZnO	38.33	0.1932	105.22
C6	30CuO:70 ZnO	48.34	0.2122	112.44
PZ	Pure ZnO	57.33	0.2344	117.87

Scanning electron microscopy (SEM) Analysis

From SEM picture (figure 3 (a) to (d)), it is observed that all the samples viz. Al_2O_3, CuO, ZnO and Sample Code C3 i.e. (15CuO:85ZnO) (optimize sample shown only) are porous in nature. Porosity varies with sample to sample and among these material, Sample Code C3 i.e. (15CuO:85ZnO) showed more porosity (small size ~ 60 to 80 nm). Due to small pores size, its surface area is more [12-14] and it shows more sensing nature. Some portion of SEM picture shows some rods with fine voids over them which helps to increase sensing properties.
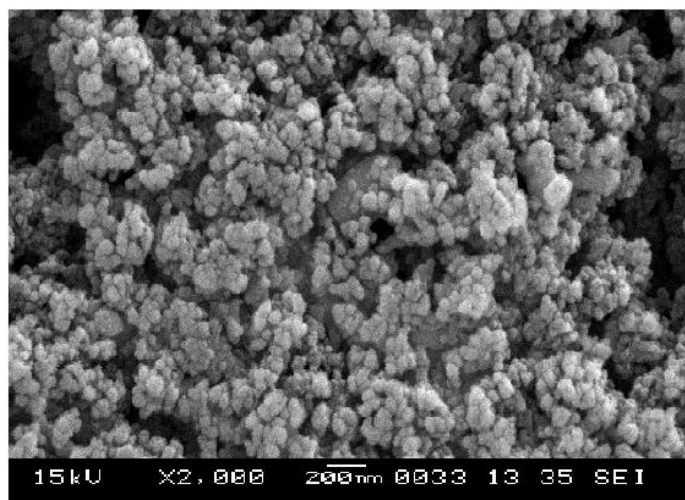

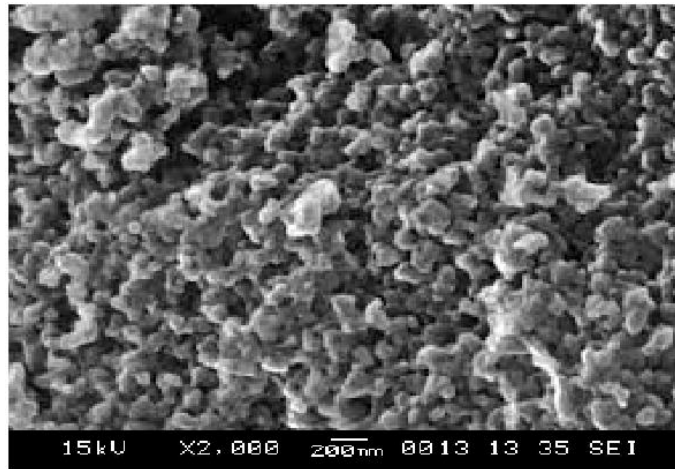**Fig. 3 (a)** SEM picture of Al_2O_3
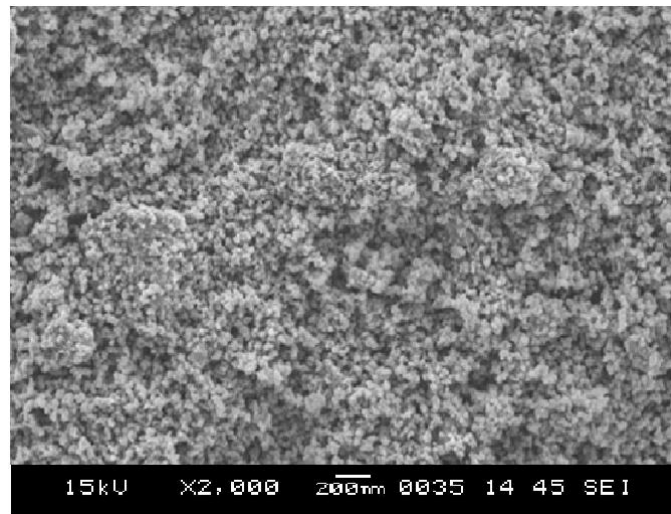
Fig. 3 (b) SEM picture of CuO

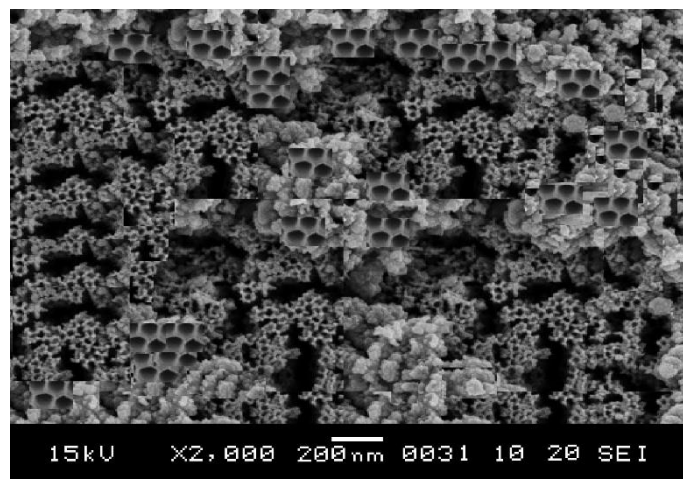**Fig. 3(c)** SEM picture of ZnO

Fig. 3 (d) SEM picture of 15CuO:85ZnO

60

Table 3. shows the average diameter and number of pores per inch of of pure Al_2O_3, CuO, and ZnO and their dopings.

Table 3. Average diameter of pore and number of pores per inch of pure samples and their dopings.

Sample Code	Pure sample and their dopings (mole %)	Average diameter of pore (nm)	Number of pores per inch (in x 2000 magnification)
PA	Al_2O_3	95	154
PC	CuO	80	172
PZ	ZnO	87	160
C1	05CuO:95ZnO	79	165
C2	10CuO:90ZnO	81	161
C3	**15CuO:85ZnO**	**45**	**245**
C4	20CuO:80ZnO	67	187
C5	25CuO:75ZnO	74	176
C6	30CuO:70 ZnO	69	183

From the SEM pictures (table 3), it is observed that Sample Code C3 i.e. (15CuO:85ZnO), have more pores per inch (calculated for x 2,000 magnification for each composition) than other sensors. Thus these sensors have more active surface areas and exhibit more sensing nature [14-15]. It is also found that average diameter of pore in case of (15CuO:85ZnO) are small as compared to other doping. This also tends to exhibit large surface area and exhibited high response of the samples.

Detection of CO_2 gas: Gas Sensing Properties

CO_2 acts as an oxidizing agent in some chemical reactions, such as the production of carbonates. It can also participate in redox reactions, where it can accept electrons and become reduced and hence its resistance increases with increase of CO_2 gas concentration [16]. The sensitivity of the sensor is given by,

$$S = \left(\frac{R_{gas} - R_{air}}{R_{air}} \right) = \left(\frac{\Delta R}{R_{air}} \right)$$

Where, R_{gas} = resistance of the sensor in presence of gas and
         R_{air} = resistance of the sensor in air

The variations of sensitivities and sensors with concentration of CO_2 gas at room temperature are shown below.
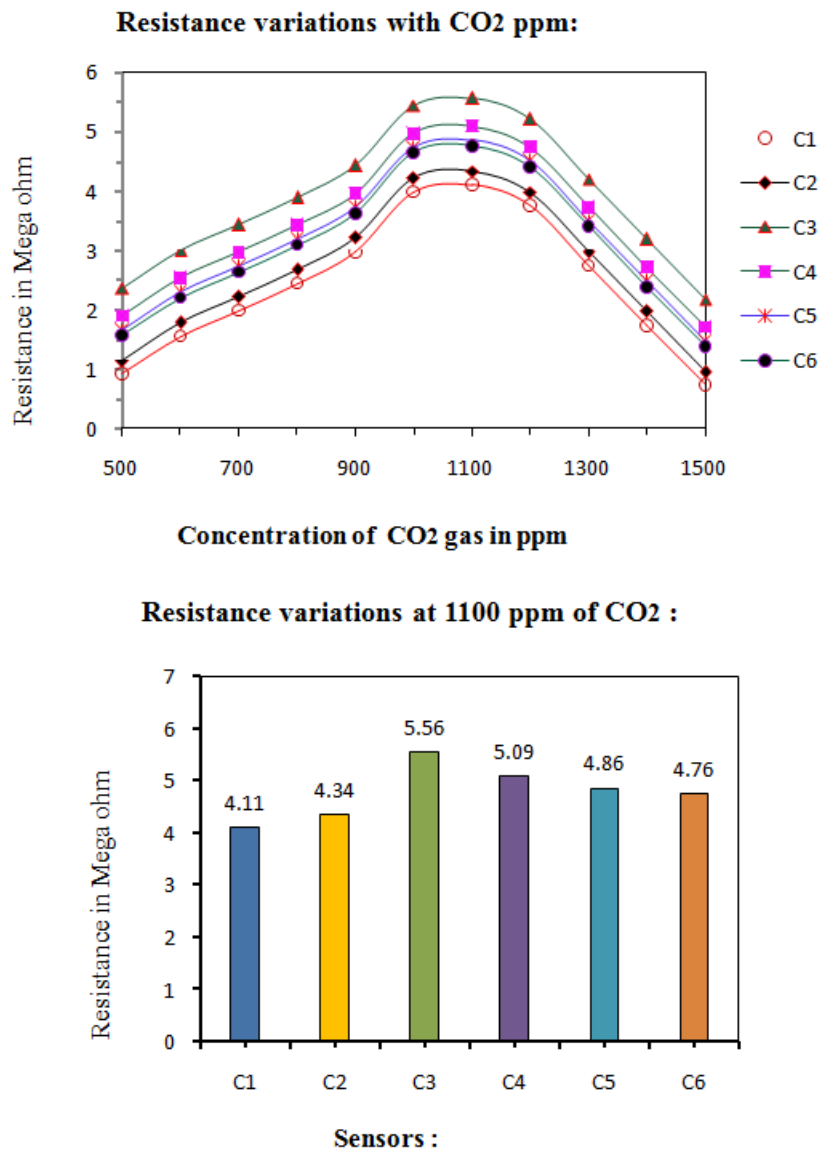
Fig. 4 : variations of resistance with CO_2 gas concentration

For CO_2 gas concentration variation from 500 ppm to 1500 ppm, variation of resistance for C1 to C6 sensors is shown in Fig. 4. As carbon-dioxide concentration increases, Cu ions interact with Zn ions by absorbing CO_2 gas and resistance increases. It is exhibited that, initially resistance increases with increases of concentration of gas, becomes maximum at 1100 ppm and then with further increase of gas concentration, it decreases. It is recorded maximum resistance for C3 sensor (15CuO:85ZnO) to be 5.56 $M\Omega$ at 1100 ppm CO_2 gas concentration [17-19].

Static Responses of sensors:

Static responses [20-21] of samples Fig. 5. of (CuO:ZnO/Al_2O_3/GP) were studied at 700, 900 and 1100 ppm of CO_2 gas concentration as a function of time and from the manifested variations, response and recovery times were calculated.
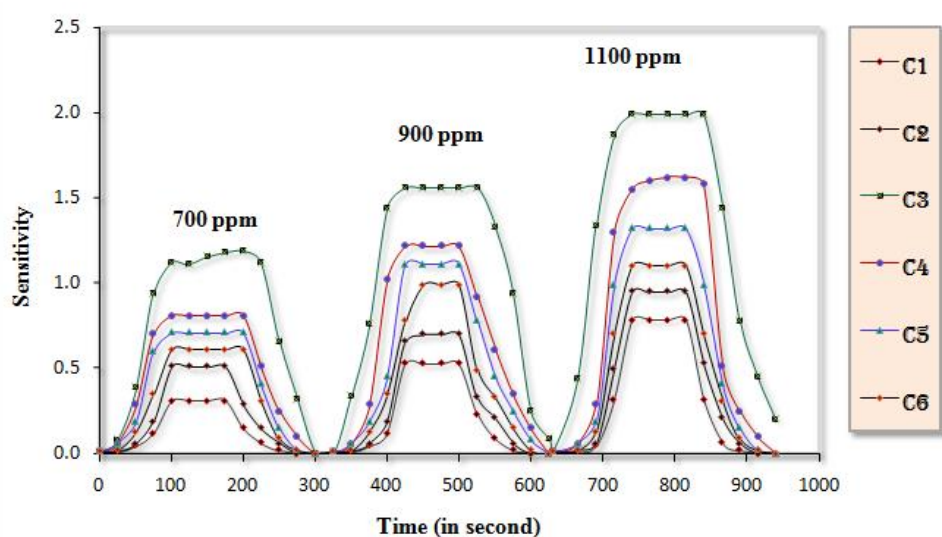
Fig. 5: Static response (response and recovery times)

Table 4. Response and Recovery times of Samples

Sr. No.	Sample Compositions	Sensor	Response time (s) for 1100 ppm	Recovery time (s) for 1100 ppm
1	05CuO:95 ZnO /Al$_2$O$_3$/GP	C1	93	95
2	10CuO:90 ZnO /Al$_2$O$_3$/GP	C2	87	89
3	15CuO:85 ZnO /Al$_2$O$_3$/GP	C3	56	61
4	20CuO:80 ZnO /Al$_2$O$_3$/GP	C4	69	76
5	25CuO:75 ZnO /Al$_2$O$_3$/GP	C5	72	79
6	30CuO:70 ZnO /Al$_2$O$_3$/GP	C6	82	91

At 100 ppm CO_2 gas concentration, from table 4, sensor C3 manifested fast response (response time 56 s and recovery time 61 s) among the fabricated sensors. Also, it is observed that response time less than that of recovery time.

CONCLUSIONS

The XRD pattern of (CuO-ZnO) system samples shows nanocrystalline form and found the desired peaks of composites. FESEM study reveals that the grain size of nanometer order and shows nano-porous structure, which leads to exhibit large surface area, stability and highest response to CO_2 gas. The response time is faster than recovery time therefore the Sample C3 i.e. (15CuO:85ZnO) is found to optimized sensor for CO_2 gas.

REFERENCES

1. Chengxiang Wang, Longwei Yin , Luyuan Zhang, Dong Xiang and Rui Gao, (20100,Review Metal Oxide Gas Sensors: Sensitivity and Influencing Factors, Sensors, 10, 2088-2106; doi:10.3390/s100302088
2. G. Korotcenkov, (2014), Handbook of Gas Sensor Materials, doi:10.1007/978-1-4614-7165-3.

63

3. Nithya Sureshkumar and Atanu Dutta,(2023) Environmental Gas Sensors Based on Nanostructured Thin Films, Multilayer Thin Films - Versatile Applications for Materials Engineering, doi.org/10.5772/intechopen. 89745

4. Quentin Simon, Davide Barreca, Alberto Gasparotto, Chiara Maccato, Eugenio Tondello, Cinzia Sada, Elisabetta Comini, Giorgio Sberveglieri, Manish Banerjee, Ke Xu, Anjana Devi, and Roland A. Fischer, CuO/ZnO Nanocomposite Gas Sensors Developed by a Plasma-Assisted Route, ChemPhysChem 0000, 00, 1 – 8, DOI: 10.1002/cphc.201101062

5. Yalu Chen, Zhurui Shen, Qianqian Jia, Jiang Zhao, Zhe Zhao, Huiming Ji, 2013, A CuO-ZnO Nanostructured p-n Junction Sensor for Enhanced N-   butanol Detection, The Royal Society of Chemistry, DOI: 10.1039/x0xx00000x

6. Ryan Dula Corpuza, Jason Rayala Albiab,2014, Electrophoretic Fabrication of ZnO/ZnO-CuO Composite for Ammonia Gas Sensing, Materials Research. 2014; 17(4): 851-856 DOI: http://dx.doi.org/10.1590/S1516-14392014005000097

7. Madhavrao K. Deore, Vishwas B. Gaikwad and Gotan H. Jain, 2016, Role of CuO-ZnO Heterojunctions in Gas Sensing Response of CuO-ZnO Thick Films, Journal of Physical Science and Application 6 (2), 51-60, doi: 10.17265/2159-5348/2016.02.008

8. K. B. Raulkar, (2019), Study on sensitivity of nano SnO_2 -ZnO composites with and without PPy layer for sensing CO_2 gas, 2019, Materials Today: Proceedings 15, 604–610.

9. Dmitry Bokov, Abduladheem Turki Jalil, Supat Chupradit, Wanich Suksatan, Mohammad Javed Ansari, 6 Iman H. Shewael, Gabdrakhman H. Valiev, and Ehsan Kianfar, (2021), Review Article, Nanomaterial by Sol-Gel Method: Synthesis and Application, Advances in Materials Science and Engineering Volume 2021, https://doi.org/10.1155/2021/5102014

10. Zahrah Alhalili, (2023), Review Metal Oxides Nanoparticles: General Structural Description, Chemical, Physical, and Biological Synthesis Methods, Role in Pesticides and Heavy Metal Removal through Wastewater Treatment, Molecules, 28, 3086. https://doi.org/10.3390/molecules28073086

11. Tai H., Wang S., Duan Z. and Jiang Y., (2020). Evolution of breath analysis based on humidity and gas sensors: Potential and challenges, Sens. Actuators B Chem., 318, 128104.

12. Nakhleh, M.K., Amal H., Jeries R., Broza Y.Y., Aboud M., Gharra A., Ivgi H., Khatib S., Badarneh S. and Har-Shai, L., (2017). Diagnosis and Classification of 17 Diseases from 1404 Subjects via Pattern Analysis of Exhaled Molecules, ACS Nano, 11, 112–125.

13. Hua B. and Gaoquan S., (2007). Gas Sensors Based on Conducting Polymers, Sensors, 7, 267-307

14. Capone S., Forleo A., Francioso L., Rella R., Siciliano P., Spada- vecchia J., Presicce D.S. and Taurino A.M. (2003), Solid state gas sensors: state of the art and future activities, Journal of Optoelectronics and Advanced Materials 5, 5, 1335 – 1348.

15. Garg R., Kumar V., Kumar D., and Chakarvarti S.K., (2015). Polypyrrole Microwires as Toxic   Gas Sensors for Ammonia and Hydrogen Sulphide, Columbia International Publishing Journal of Sensors and Instrumentation, 3, 1-13.

16. Arindam Das and Dipankar Panda ,(2019), SnO_2 Tailored by CuO for Improved CH_4 Sensing at Low Temperature, Advanced Science News, Phys. Status Solidi B, 1800296, DOI: 10.1002/pssb.201800296

17. Capone S., Forleo A., Francioso L., Rella R., Siciliano P., Spada- vecchia J., Presicce D.S. and Taurino A.M. **(2003),** Solid state gas sensors: state of the art and future activities, Journal of Optoelectronics and Advanced Materials 5, 5, 1335 – 1348.

18. Garg R., Kumar V., Kumar D., and Chakarvarti S.K., **(2015)**. Polypyrrole Microwires as Toxic   Gas Sensors for Ammonia and Hydrogen Sulphide, Columbia International Publishing Journal of Sensors and Instrumentation, 3, 1-13.

19. Lin C.W., Chen H.I., Chen T.Y., Huang C.C., Hsu C.S., Liu R.C. and Liu W.C. **(2011)**, Ammonia Gas Sensing Performance of an Indium Tin Oxide (ITO) Based Device with an Underlying Au-Nanodot Layer, Sens Actuators B 160:1481.

20. Shang Y., Wang X., Xu E., Tong C. and Wu J. **(2015)**, Porous Silicon Structures as Optical Gas Sensors, Anal Chim Acta, 15(8), 19968–19991.

21. Wang Y., Jia W., Strout T., Schempf A., Zhang H., Li B., Cui J. and Lei Y., **(2009)**, Preparation, Characterization and Sensitive Gas Sensing of Conductive Core-sheath TiO_2-PEDOT Nanocables, Sensors (Basel), 9(9), 6752–6763.

64